262 *J. Chem. Eng. Data* **2010,** *55,* 262–266

Experimental Investigation of Methane Hydrates Equilibrium Condition in the Presence of KNO_3, $MgSO_4$, and $CuSO_4$

Lutz O. Porz,[†] **Matthew A. Clarke,*** **and Lothar R. Oellrich**[†]

Department of Chemical & Petroleum Engineering, University of Calgary, 2500 University Drive, Calgary, Alberta, Canada, T2N 1N4

A new isochoric reactor was commissioned for studying gas hydrate equilibrium formation, and experiments were carried out to measure the equilibrium conditions for methane hydrate formation in aqueous solutions of $CuSO_4$, KNO_3, and $MgSO_4$. The experimental conditions ranged from (273 to 281) K in temperature and between (3 and 6) MPa in pressure, and the mass fraction of salt ranged from (0.025 to 0.402), depending on the salt. In the case of all three salts, it was observed that there was an inhibiting effect on the hydrate formation, which is in contrast to a previous observation that found $CuSO_4$ had a promoting effect on CO_2 hydrates.

Introduction

Hydrates, properly called clathrate hydrates, are icelike structures with water and small guest molecules that are formed at low temperatures and elevated pressure. Several different hydrate formers have been identified such as carbon dioxide, hydrogen sulfide, nitrogen, oxygen, xenon, krypton, chlorine, and natural gas components such as methane, ethane, propane, etc. and their mixtures. At a microscopic level, the water molecules build a crystalline lattice, wherein the guest molecule is entrapped via van der Waals forces. Gas hydrates can exist in one of four crystal structures, depending on the temperature, pressure, and composition of the guest molecules: two cubic structures called structure I and II,[1,2] structure H (a hexagonal structure),[3,4] and a fourth structure known as structure T (a trigonal structure).[5]

Gas hydrates have been known to the scientific and to the industrial community for many years, originally as a nuisance that was to be avoided, whereas recently they have gained the spotlight for their ability to store a large amount of gas. One cubic meter of hydrate can contain up to 160 m^3 of gas at standard conditions.[2] Thus, hydrates have garnered attention because of their potential use as a means to store gas. This stored gas could subsequently be used for meeting peak load gas demand.

While the potential for gas hydrates as a storage medium has been recognized,[6−8] there are still many technical issues that need to be addressed before this technique reaches wide-scale commercialization. One of the important issues involved in using gas hydrates as a medium for gas storage is minimizing the compression costs, by lowering the required pressure for gas hydrate formation. To date researchers have found that forming gas hydrates in Tetrahydrafuran[9] as well as forming semiclathrates in tetrabutylammonium bromide[10] can lower the required pressure for gas hydrate formation. In 2004, the group of Bishnoi[11] observed that the formation pressure for CO_2 hydrates in aqueous $CuSO_4$ was lower than the corresponding formation pressure in pure water. The initial impetus for examining hydrate formation in $CuSO_4$, $MgSO_4$, and KNO_3 was due to the fact that in all three cases the osmotic coefficient of these salts exhibited a minimum.

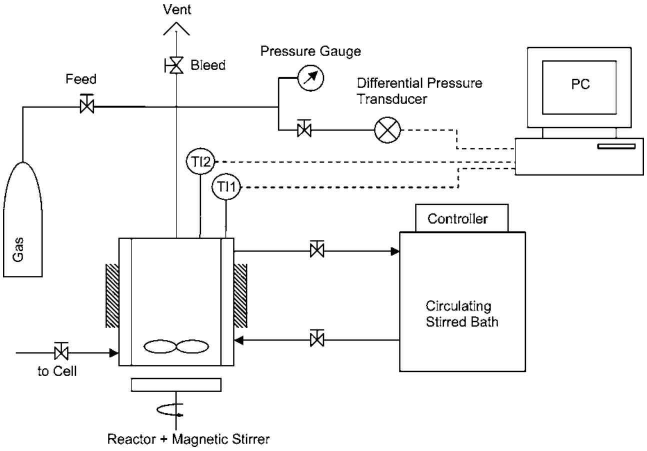

Figure 1. Flow diagram of the experimental apparatus.

As a follow-up to the aforementioned study, a subsequent study has been initiated to observe the effects of $CuSO_4$, $MgSO_4$, and KNO_3 on the formation pressure for methane gas hydrates. Additionally, a new apparatus was commissioned to obtain the experimental data. This project was one piece of a larger proposed study that is concerned with experimental and numerical modeling issues to the thermodynamics of phase behavior of gas hydrates at the University of Calgary. Results of this work could advance the design and optimization of processes that employ gas hydrates, such as gas storage systems.

Experimental Apparatus, Materials, and Procedure

Apparatus. A new experimental apparatus was commissioned for this experiment. At the heart of the new apparatus is a sapphire-tube reactor, which was originally built by Parent and Bishnoi.[12] For the current study, the jacketed reactor was connected to a programmable cooling bath. Figure 1 shows a schematic for the experimental apparatus, and Figure 2 is a mechanical drawing of the cell and flange.

---

* Corresponding author. E-mail: maclarke@ucalgary.ca.

[†] Address: Institut für Technische Thermodynamik and Kätetechnik, Universität Karlsruhe, Germany.

10.1021/je9003228 CCC: $40.75

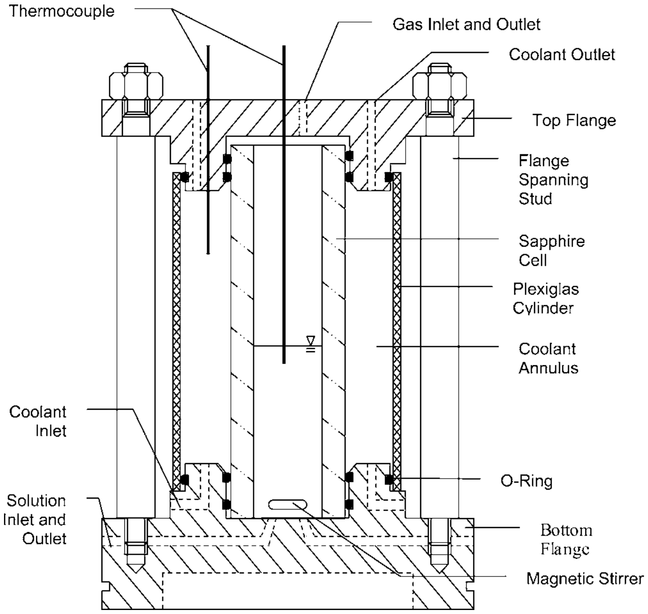

Figure 2. Schematic drawing from the reactor.

The reactor itself is a sapphire tube (3/4 in. inside diameters × 1−1/4 in. outside diameter × 4−1/2 in. long) that is placed inside a concentric plexiglas cylinder. Both cylinders are held by top and bottom stainless steel flanges. Three flange spanning studs are used to fix the sapphire tube and the two flanges together. The reactor is constructed in such a way that only minimal axial and radial stress is transmitted to the sapphire cell when it is assembled. The sapphire tube, which was made of optical clarity with a random crystal orientation, was designed for working pressures in excess of 20 MPa at temperatures between (250 and 400) K. A magnetic stir bar is placed inside the sapphire tube to ensure an intensive agitation, and it is driven by a rotating magnet, which is placed under the reactor.

In the space between the sapphire tube and the outer plexiglass tube, a 50/50, by volume, mixture of ethylene glycol and water flows at a constant volumetric flow rate. The coolant flows in a continuous loop between the reactor assembly and an external programmable cooling bath. The temperature of the flowing coolant is controlled from the cooling bath, and the entire assembly is insulated to minimize heat transfer from the surroundings. The pressure in the reactor was measured using a (4 to 20) mA differential pressure transducer, and the reactor and cooling jacket temperature were measured using type-T thermocouples (TI1 and TI2 in Figure 1). The span of the differential pressure transducer is 11 MPa with an uncertainty of 0.25 % of the full span. The thermocouples are calibrated in the range of (269 to 293) K with a standard deviation of the least-squares fit of 0.025 K. The signals from the pressure transducer and the thermocouples are fed through a field-point data acquisition unit from where they are subsequently fed via a USB connection into a computer. The data are then written

Table 1. Experimental Data of Methane Hydrate Equilibrium in Aqueous KNO_3 Solutions

mass fraction of salt ($\times 10^2$)	T/K	p/MPa
2.497	273.75	2.936
	276.08	3.687
	278.2	4.638
	280.81	5.982
9.308	273.95	3.177
	275.46	3.802
	278.15	4.934
	280.07	5.964

Table 2. Experimental Data of Methane Hydrate Equilibrium in Aqueous $MgSO_4$ Solutions

mass fraction of salt ($\times 10^2$)	T/K	p/MPa
15.31	273.5	3.014
	275.79	3.689
	278.43	4.665
	280.55	6.024
28.00	274.12	3.338
	276.08	4.068
	278.04	5.039
	279.57	6.025
40.17	273.85	3.98
	274.55	4.374
	276.00	5.199
	277.3	5.914

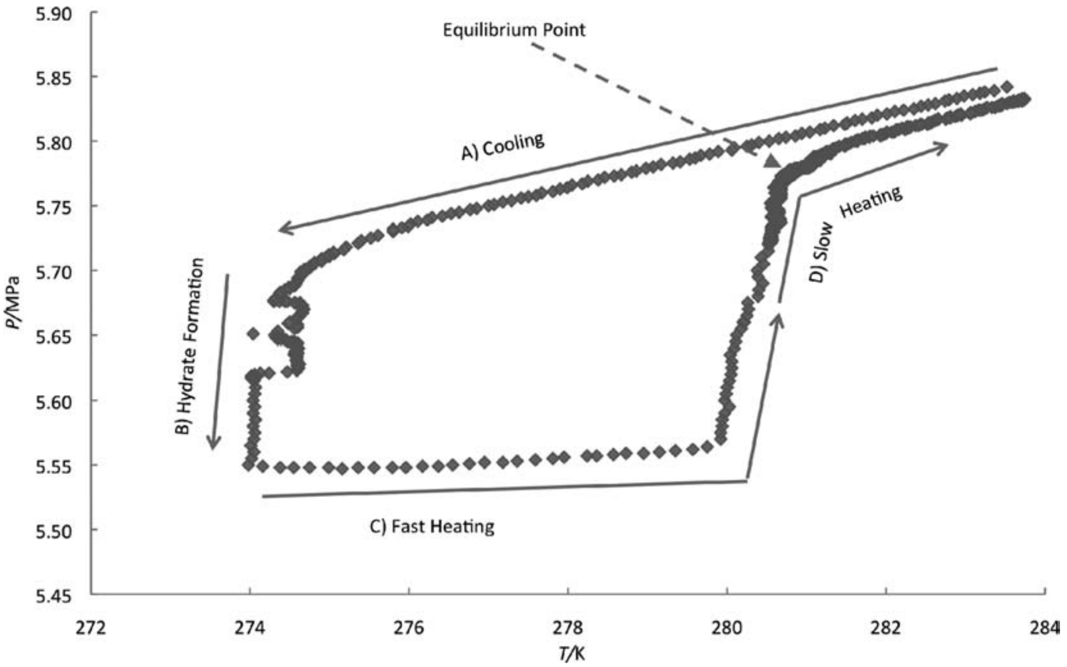

Figure 3. Typical experimental pressure−temperature trajectory (CH_4 hydrates formed in 0.075 mass fraction aqueous $CuSO_4$).

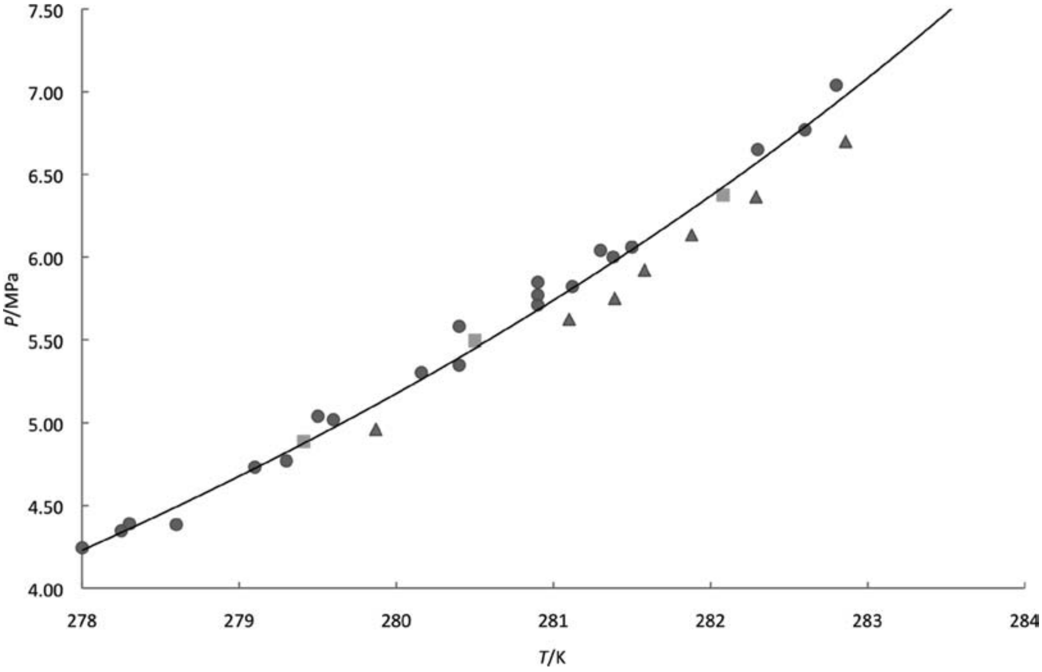

Figure 4. Methane hydrate equilibrium data in pure water, obtained from the current study compared to published data. ■, This work with continuous heating. ▲, This work with stepped heating. −, Predictions from HYCAL. ●, Published data taken from the compilation of Sloan.[4]

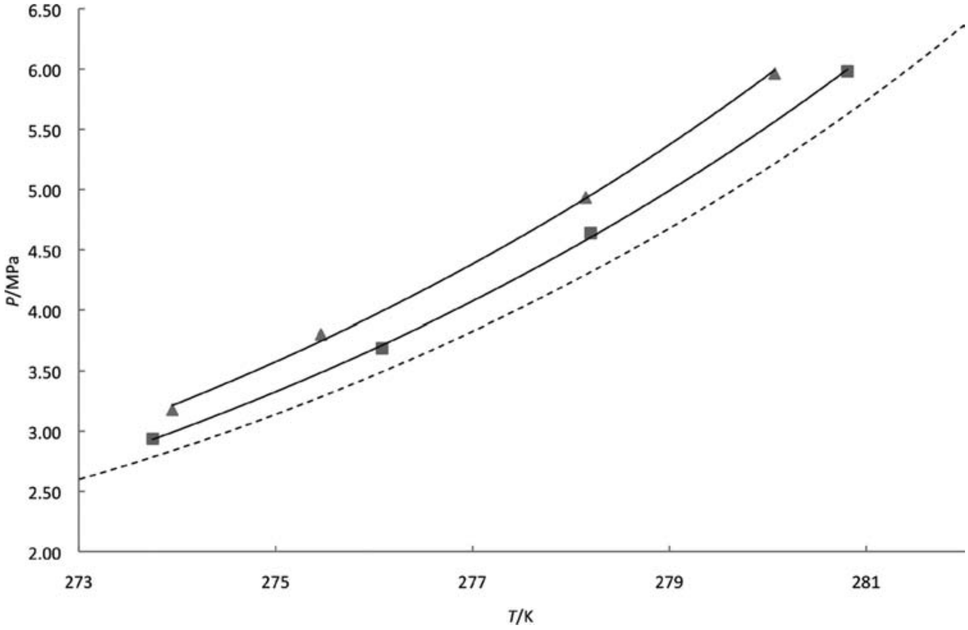

Figure 5. Methane hydrate equilibrium conditions in aqueous KNO_3. ■, Experimental data for methane hydrate in 0.02497 mass fraction aqueous KNO_3. ▲, Experimental data for methane hydrate in 0.09308 mass fraction aqueous KNO_3. −, Visual fit of experimental data. - - -, HYCAL predictions of methane hydrate equilibrium conditions in pure water.

to file every thirty seconds. The pressure transducer was calibrated using a dead-weight tester, and the thermocouples were calibrated using a precision thermometer.

Materials and Procedure. The gas used for the experiments was methane, with a purity of 99.97 % supplied from PRAXAIR.

Solutions were prepared by mass, using an electronic balance (Mettler) with a readability of 0.01 g. Anhydrous cupric sulfate (99.0 % $CuSO_4$), magnesium sulfate heptahydrate [(98.0 to 102.0) % $MgSO_4 \cdot 7H_2O$], potassium nitrate (99.0 % KNO_3) (all supplied by MERCK) were added to demineralized water to prepare respective experimental solutions.

Before each series, the cell was rinsed several times with demineralized water and then once with the experimental solution. The system was flushed three times with methane. An amount of 12 mL of the aqueous solution was injected to the cell.

The procedure that was used for the experiments is based on the isochoric procedure used at the Universität Karlsruhe in the group of Professor Oellrich,[13−15] and a pressure−temperature trajectory for a typical experiment can be seen in Figure 3. In this procedure, the system was initially cooled with a fast cooling rate ($-10\ K \cdot h^{-1}$) from an initial point outside of the hydrate stability zone to a point that is well within the hydrate stability zone. This stage corresponds to section A in Figure 3. During the cooling phase, pressure decreases with temperature in an almost linear trend until the point at which hydrates appear. At

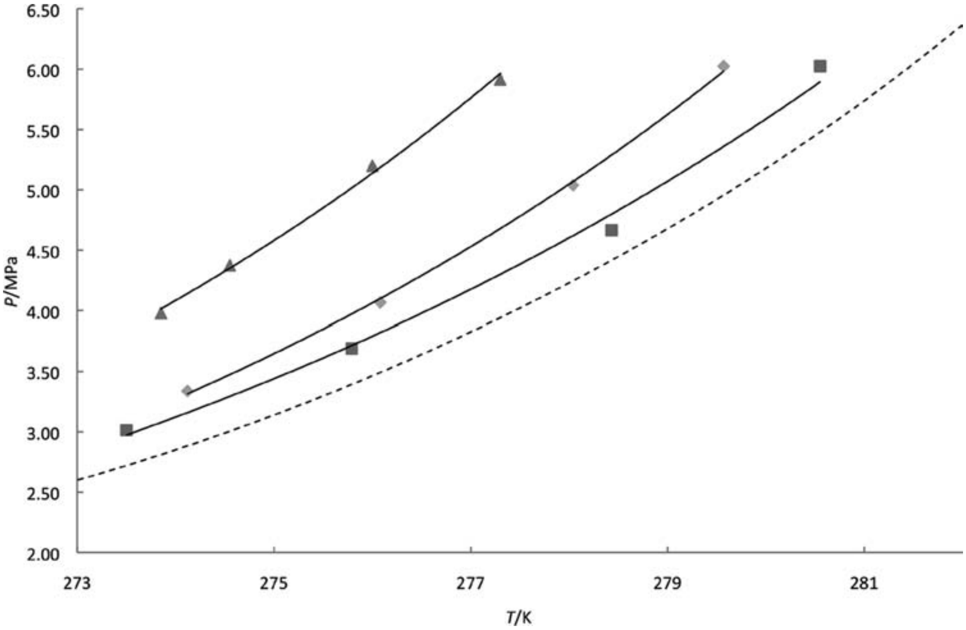

Figure 6. Methane hydrate equilibrium conditions in aqueous $MgSO_4 \cdot 7H_2O$. ■, Experimental data for methane hydrate in 0.1531 mass fraction aqueous $MgSO_4 \cdot 7H_2O$. ♦, Experimental data for methane hydrate in 0.2800 mass fraction aqueous $MgSO_4 \cdot 7H_2O$. ▲, Experimental data for methane hydrate in 0.4017 mass fraction aqueous $MgSO_4 \cdot 7H_2O$. −, Visual fit of experimental data. - - -, HYCAL predictions of methane hydrate equilibrium conditions in pure water.

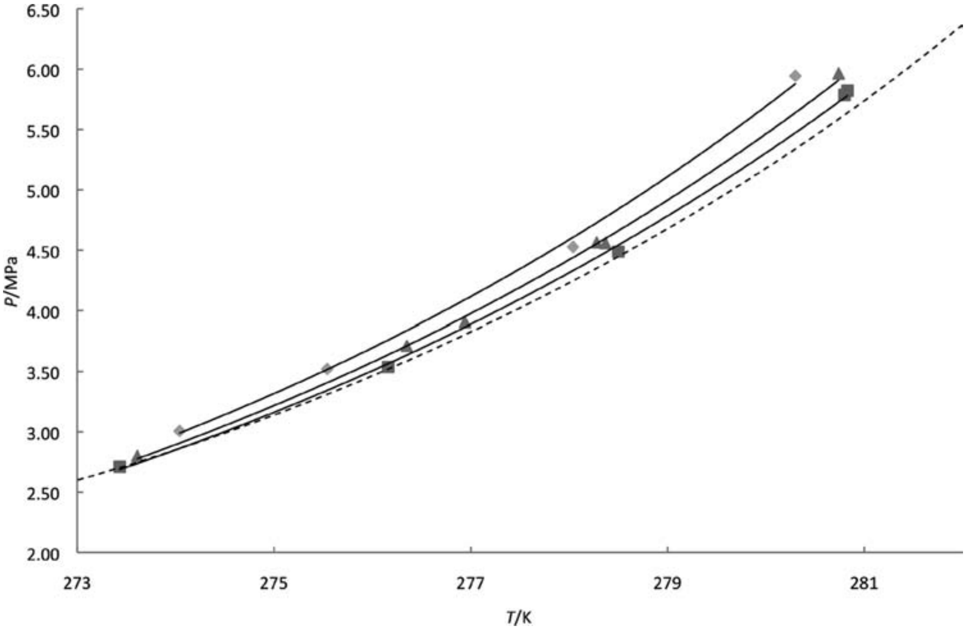

Figure 7. Methane hydrate equilibrium conditions in aqueous $CuSO_4$. ■, Experimental data for methane hydrate in 0.0750 mass fraction aqueous $CuSO_4$. ▲, Experimental data for methane hydrate in 0.1110 mass fraction aqueous $CuSO_4$. ♦, Experimental data for methane hydrate in 0.1250 mass fraction aqueous $CuSO_4$. −, Visual fit of experimental data. - - -, HYCAL predictions of methane hydrate equilibrium conditions in pure water.

the onset of hydrate formation, the solution changed from clear to opaque, and the pressure decreased as gas was consumed by the growing hydrate crystals (section B in Figure 3). After hydrate formation had been observed, the system was heated, initially at a high rate of heating ($+10\ K \cdot h^{-1}$). This corresponds to section C in Figure 3. Once the point was reached at which the pressure began to increase sharply, the rate of heating was significantly reduced. A slow heating phase (section D in Figure 3) was subsequently initiated in which the temperature was stepped up in increments of $+0.1\ K \cdot h^{-1}$. At each increment, the system was given sufficient time to stabilize before the temperature was again increased. Stepped heating continued until the temperature returned to the initial temperature. In an isochoric experiment, the equilibrium point is found as the pinch point in the heating curve.[13] Finally, as this was the inaugural study with this equipment, preliminary experiments were conducted to verify the accuracy of the equipment; this will be presented in the following section.

Results and Discussion

Validation of Apparatus. For the purpose of validating the experimental apparatus and procedure, the results for a well-studied system were reproduced, that system being methane hydrates in pure water. Additionally, in the validation study, the effect of continuous heating versus stepped heating was also observed. Experimental data were obtained with methane and

Table 3. Experimental Data of Methane Hydrate Equilibrium in Aqueous $CuSO_4$ Solutions

mass fraction of salt ($\times 10^2$)	T/K	p/MPa
7.5	273.43	2.711
	276.16	3.537
	278.5	4.488
	280.8	5.788
	280.83	5.822
11.1	273.61	2.8
	276.35	3.711
	276.94	3.908
	278.28	4.564
	278.37	4.558
	280.74	5.965
12.5	274.04	3.007
	275.54	3.52
	278.04	4.527
	280.3	5.944

pure water in a pressure range from (4.9 to 6.7) MPa and between (279 and 283) K. Equilibrium conditions from this work compared to literature data can be seen in Figure 4. As shown in Figure 4, the stepped heating method is able to excellently reproduce the existing experimental data. Thus, the step-heating method was used for later experiments.

Experimental Results and Discussion. Methane hydrate equilibrium conditions in the presence of aqueous KNO_3, $MgSO_4$, and $CuSO_4$ are presented in Tables 1, 2, and 3 and Figures 5, 6, and 7. Solid lines are visual fit curves to clarify the trend of the equilibrium points, whereas the dotted line represents the methane hydrate formation prediction with pure water as calculated by HYCAL, which is a commercial process simulator. From the graphs, it can be seen that all three salts have a pronounced inhibiting effect and that this inhibiting effect increases as the concentration of the salt increases. This is not entirely surprising for the case of the aqueous KNO_3, $MgSO_4$ solutions, since it was also observed that these salts inhibit CO_2 hydrate formation.[11] However, the results for methane hydrates in $CuSO_4$ were particularly surprising when viewed in conjunction with the study of Clarke et al.[11] in which they observed that $CuSO_4$ had a promoting effect on the formation of CO_2 hydrates. At this point, it is not entirely clear as to why $CuSO_4$ had a promoting effect on CO_2 hydrates and an inhibiting effect on CH_4 hydrates.

One hypothesis as to why this result was observed with CO_2 is based upon the behavior of the aqua ion ($[Cu(H_2O)_6]^{2+}$) when it interacts with the dissolved CO_2. It is known that addition of ligands to aqueous solutions leads to the formation of complexes by successive displacement of water molecules.[16] For example, Cotton et al.[16] reported that when NH_3 is dissolved in water the complex ($[Cu(NH_3)(H_2O)_5]^{2+}$) is formed.

Conclusions

Experiments were conducted in a new apparatus to measure the effect of aqueous KNO_3, $MgSO_4$, and $CuSO_4$ on methane hydrate formation. After the new apparatus was validated by reproducing reported values for methane hydrate formation pressures in pure water, experiments were conducted with the aforementioned salts in a pressure range of (3 to 6) MPa, in a temperature range between (273 and 281) K, and salt mass fractions between (0.025 and 0.402). It was found that in the case of all three salts an inhibiting effect was observed and that this inhibiting effect increased as the salt concentration in solution increased.

Acknowledgment

The authors would like to thank Dr. Christoph Windmeier for his useful advice in standardizing the experimental procedure.

Literature Cited

(1) von Stackelberg, M.; Müller, H. R. Feste Gas Hydrate II. *Z. Elektrochem.* **1954**, *58*, 25–39.

(2) Makogan, Y. F. *Hydrates of Natural Gas*; Penn Well Books: Tulsa, 1981.

(3) Ripmeester, J. A.; Ratcliffe, C. I.; Tse, J. S. The Nuclear Magnetic Resonance of 129Xe Trapped in Clathrates and Some Other Solids. *J. Chem. Soc., Faraday Trans.* **1988**, *84*, 3731–3739.

(4) Sloan, E. D., Jr. *Clathrate Hydrates of Natural Gases*, 2nd ed. rev. and expanded; Marcel Dekker Inc.: New York, 1998.

(5) Udachin, K. A.; Ratcliffe, C. I.; Ripmeester, J. A. A Dense and Efficient Clathrate Hydrate Structure with Unusual Cages. *Angew. Chem.* **2001**, *113*, 1343–1345.

(6) Kalogerakis, N.; Jamaluddin, A. K. M., Dholabhai, P., Bishnoi, P. R. Effect of Surfactants on Hydrate Formation Kinetics. *Proceedings of the 1993 SPE International Symposium on Oilfield Chemistry*; 1993; pp 375−383.

(7) Sun, Z.; Wang, R. Z.; Ma, R. S.; Guo, K. H.; Fan, S. S. Natural Gas Storage in Hydrates with the Presence of Promoters. *Energy Conversion Manage.* **2003**, *44*, 2733–2742.

(8) Rogers, R.; Zhong, Y.; Etheridge, J. A.; Arunkumar, R.; Pearson, L. E.; Hogancamp, T. K. Micellar Gas Hydrate Storage Process. *Proceedings of the Fifth International Conference on Gas Hydrates*; Trondheim, Norway, June 13−16, 2005, 2005; pp 1361−1365.

(9) Linga, P.; Adebola, A.; Englezos, P. Medium-pressure clathrate hydrate/membrane hybrid process for post-combustion capture of carbon dioxide. *Environ. Sci. Technol.* **2008**, *42*, 315–320.

(10) Ichiro, T.; Shingo, T. Storage and transport of cold using clathrate hydrate slurries: Fundamental thermophysical characteristics of aqueous solution of TBAB. *Proceedings of the Intersociety Energy Conversion Engineering Conference*; 2001; Vol. 2, pp 695−700.

(11) Clarke, M. A.; Majumdar, A.; Bishnoi, P. R. Experimental Investigation of Carbon Dioxide Hydrate Formation Conditions in the Presence of KNO_3, $MgSO_4$ and $CuSO_4$. *J. Chem. Eng. Data* **2004**, *49*, 1436–1439.

(12) Parent, J. S.; Bishnoi, P. R. Investigations into the nucleation behaviour of methane gas hydrates. *Chem. Eng. Commun.* **1996**, *144*, 51–64.

(13) Nixdorf, J.; Oellrich, L. R. Experimental determination of hydrate equilibrium conditions for pure gases, binary and ternary mixtures and natural gases. *Fluid Phase Eqilib.* **1997**, *139*, 325–333.

(14) Rock, A. Experimentelle und theoretische Untersuchung zur Hydratbildung aus Ggemischen in inhibitorhaltigen wässrigen Lösungen; Dissertation, Universität Karlsruhe (TH), 2002.

(15) Windmeier, C. Experimentelle und theoretische Untersuchungen zum Phasen- und Zersetzungsverhalten von Gashydraten; Dissertation, Universität Karlsruhe (TH), 2009.

(16) Cotton, F. A.; Wilkinson, G.; Gaus, P. L. *Basic Inorganic Chemistry*, 3rd. ed.; Wiley and Sons: New York, 1995.

Received for review April 1, 2009. Accepted May 30, 2009. The funding for this work was provided by the Zandmer Estate in the Department of Chemical & Petroleum at the University of Calgary.

JE9003228